

## Microsecond time scale lateral-mode dynamics in a narrow stripe InGaN laser

Christoph Eichler

*Optoelectronics Department, University of Ulm, 89069 Ulm, Germany*

Daniel Hofstetter

*Institute of Physics, University of Neuchâtel, 2000 Neuchâtel, Switzerland*

Weng W. Chow

*Sandia National Laboratories, Albuquerque, New Mexico 87185-0601*

Stephan Miller, Andreas Weimar, Alfred Lell, and Volker Härle

*OSRAM Opto Semiconductors, 93049 Regensburg, Germany*

Time-resolved measurements of the spectrum and the far field of InGaN-based laser diodes show lateral-mode changes and gradual tilting of the far field on a microsecond time scale. Numerical simulations based on a microscopic theory are in good agreement with the measurements. The observed effects are attributed to lateral carrier diffusion in combination with thermal lensing.

For violet-blue diode lasers, there exist several important applications, such as optical storage and laser printing, requiring lateral mode stability. While the design of single-mode lasers is an ongoing problem, the underlying physical mechanisms leading to stable fundamental-lateral mode operation in conventional semiconductor lasers is, in principle, well understood. However, this understanding may not apply to the wide-band-gap group-III nitride (III-N) material system because of its drastically different physical properties.<sup>1</sup> That this is indeed the case is demonstrated in our recent observation of lateral-mode instabilities on a microsecond time scale in a narrow (2.25  $\mu\text{m}$  wide) ridge-waveguide InGaN laser.

The investigated laser diodes were fabricated by OSRAM Opto Semiconductors. They were grown on a SiC substrate without ELO techniques by metalorganic chemical vapor deposition and consist of a 560 nm thick AlGaIn:Si cladding, followed by a 120 nm GaN:Si lower waveguide layer, three 2 nm  $\text{In}_{0.1}\text{Ga}_{0.9}\text{N}/\text{GaN}$  quantum wells with GaN:Si barriers, an  $\text{Al}_{0.2}\text{Ga}_{0.8}\text{N}$  electron blocking layer, a 100 nm thick GaN:Mg upper waveguide layer, and a 400 nm thick AlGaIn:Mg upper cladding layer. Contacts are deposited on a *p*-GaN cap layer on top of the ridge and on the *n*-SiC backside. The cleaved facets are coated with high reflectivity coating ( $R \sim 98\%/70\%$ ).<sup>2</sup> The devices are operated in junction side up configuration, which is possible due to the SiC substrate. Since we use short pulses in the microsecond range, the back contact of the device does not see a temperature increase during the pulse, as shown in Ref. 3. After each pulse, the laser has enough time to cool down again due to the very low duty cycle. Thus, the kind of mounting the device onto the heatsink has only negligible influence on the effects described in this letter.

For measurements of the time-resolved optical spectrum, the light of the temperature stabilized laser diode is collimated and then focused on the entrance slit of a grating monochromator. At the output slit, the light of the actually

selected wavelength is collected by a fast photomultiplier tube. Thus, for this particular wavelength the intensity distribution versus time can be observed on an oscilloscope connected to the photomultiplier tube. Scanning the selected wavelength of the monochromator over the range of the emission spectrum of the laser diode yields therefore a three-dimensional graphics with time and wavelength as the *x* and *y* axis, respectively, and optical intensity as the *z* axis (color encoded). This plot, which is shown in Fig. 1 (top), allows to observe the evolution of the laser spectrum during a current pulse. The corresponding time-resolved far field is measured in the same manner. The only difference to the previous measurement is that the monochromator is now replaced by a step motor controlled arm which moves the pigtail of a multimode fiber on a circular path around the emitting facet of the laser diode. The light collected by the fiber is again measured by the photomultiplier tube. An example of such a far-field measurement is shown in Fig. 1 (bottom).

In order to get some insight into the mechanism of their modal behavior, we analyzed laser diodes with different ridge widths and at different measurement conditions. A typical spectrum and far field of a 2.25  $\mu\text{m}$  wide stripe laser is shown in Fig. 1. In this case, current pulses of 9  $\mu\text{s}$  length at a very low duty cycle of 0.1% were used to excite the laser. Let us first concentrate on Fig. 1 (left). It is evident that the laser turns on and immediately starts to heat up, as indicated by the large wavelength shift. After approximately 1  $\mu\text{s}$ , the wavelength shift slows down, indicating that the laser diode has reached an almost constant temperature distribution. Beyond this point, the effect of the heat capacity of the materials round the active area becomes less important and the temperature increase is dominated by the internal thermal resistance of the device.<sup>3</sup> The far field also shows a small change within the first microsecond, but then stays constant for the rest of the pulse. For slightly higher currents (Fig. 1 middle) and after approximately 1  $\mu\text{s}$  the laser enters a transition regime: A second wavelength starts to appear and an

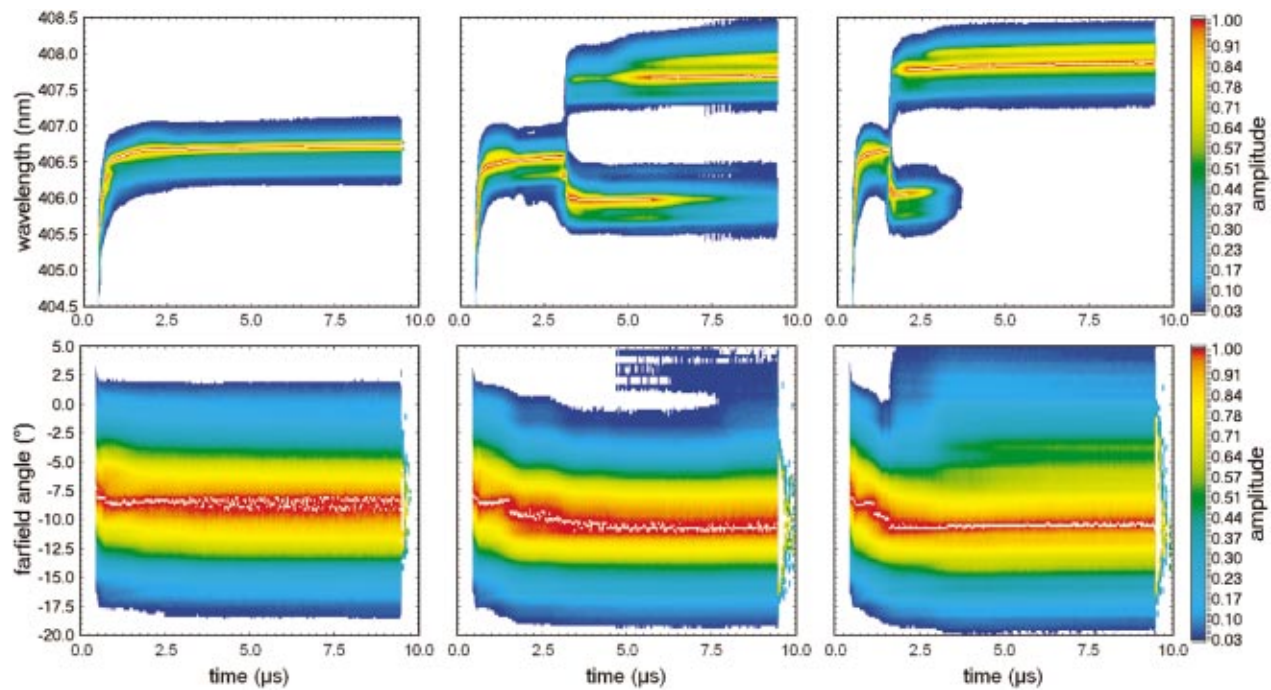


FIG. 1. (Color) A  $2.25 \mu\text{m}$  wide InGaN-laser diode at injection currents of  $1.08I_{\text{th}}$  (left),  $1.16I_{\text{th}}$  (middle), and  $1.20I_{\text{th}}$  (right). The spectrum becomes bimodal at higher currents and the far field shows a pronounced beam-steering effect.

increasingly asymmetric far-field distribution is observed. After a certain time ( $2.66 \mu\text{s}$ ) which is characteristic for this particular injection current density, the laser shows an abrupt change in both the spectral and the far-field behavior. Beyond this point, it lases suddenly in two lateral modes. This behavior is even more pronounced when the current density is further increased. As shown in Fig. 1 (right), the splitting into two modes occurs already after  $1.11 \mu\text{s}$ . In pulsed  $L$ - $I$  curves, this mode switching is clearly visible as a kink.

There exist two possible explanations for the mode switching: one is the temperature induced change of the refractive index. Since the number of guided modes  $m$  depends on the difference between the refractive index of the waveguide  $n_f$  and the surrounding material  $n_s$ ,<sup>4</sup> a temperature rise underneath the ridge results in an increase of the refractive index, leading to a better guiding of higher order modes. However, since the highest temperature is found in the center of the ridge, the resulting refractive index change alone is not sufficient to explain the tilting of the far field.

To explore as to whether the experimental observations can also originate from intrinsic properties of the III-nitride material system, the laser structure is modeled using the coupled Maxwell-semiconductor-Bloch equations. These equations treat the wave-optical (diffractive) aspect of the intracavity laser field, and provide a microscopic description of InGaN quantum-well susceptibility.<sup>1</sup> We numerically solve these equations simultaneously with a partial differential equation ( $x$ ,  $z$ , and  $t$ ) that accounts for carrier diffusion effects on the total carrier density spatial distribution. Figure 2 shows (from left to right) the changes in the laser field with increasing injection current. The top two rows depict the lateral laser field intensity and phase at the output facet. Note the abrupt transition from a plane phase front to one with appreciable tilt. A consequence of the phase-front tilt is beam steering as evident from the lateral displacement of the far-

field intensity maximum (see third row, Fig. 2).

The theoretical results may be traced to the coexistence of carrier-induced refractive index change and lateral carrier diffusion. Basically, an increase in injection current gives rise to a broader pumped region at the quantum well because of increased lateral carrier diffusion. The effects of this active region broadening is accentuated by spatial hole burning, which in a semiconductor causes an increase in the index guiding of the intracavity mode. The combination of a wider gain region and a stronger index confinement leads to the transition from operation with the fundamental mode to one with a tilted single-lobe mode. Our simulations show that the onset of tilted mode operation depends on the filamentation (self-focusing) strength of the quantum-well (QW) gain structure. Compared to typical near-infrared QW lasers,

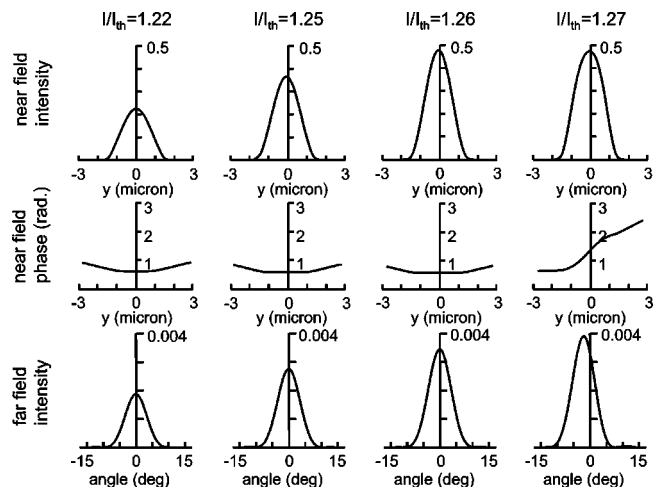


FIG. 2. Near field intensity, near field phase, and far-field distribution of InGaN laser diodes at different currents. In the far field, a tilt of about  $-2^\circ$  is clearly visible for a current of  $1.27I_{\text{th}}$ . For smaller currents, no tilt can be observed.

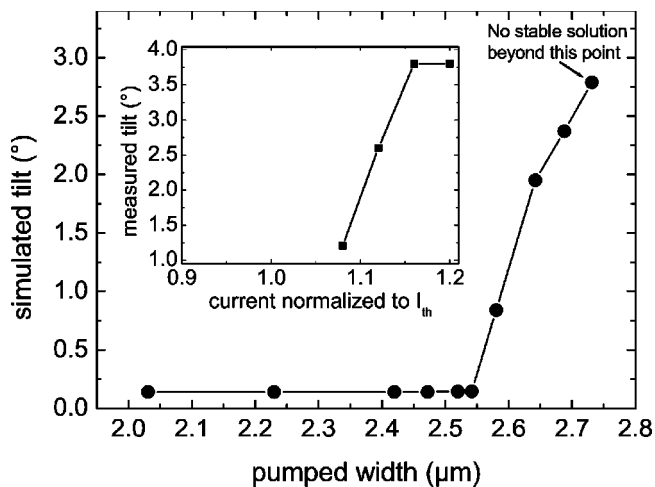


FIG. 3. Simulated far-field tilt as a function of effectively pumped width. Beyond a pumped width of about  $2.5 \mu\text{m}$ , a tilt can be observed. The inset shows measured tilt values as a function of current.

the antiguiding (self-focusing) factor  $R$  in 2 nm InGaN quantum wells is a factor of 3 higher, primarily because of the significantly heavier electron and hole effective masses in nitride semiconductors.<sup>1</sup>

We also find a direct correspondence between beam steering and the effective pumped width as indicated in Fig. 3. The effective pumped width is the full width at half maximum of the computed carrier distribution at the quantum well, where the difference between this width and the stripe width is due to lateral carrier diffusion during carrier transport from the electrodes to the quantum well. The curve shows qualitative agreement with the experiment (compare with inset), and that beam steering occurs only when the pumped width exceeds a certain critical value. For too small a pumped region ( $1.5 \mu\text{m}$  for our laser structure), the waveguide loss of the tilt mode is too large; therefore such a mode cannot survive. Note also that beyond a certain width there exists no stable solution, which marks the onset of multimode operation. The time-averaged tilt angle is unlikely to

further increase with multimode operation. Correspondingly, in the experiment, we observed a saturation of the far-field tilt.

Further experiments have shown that if the stripe width is much larger than the critical value, the laser starts already to oscillate in a higher order lateral mode and shows multiple mode transitions during a pulse. In agreement with literature data, we found that for single mode operation the ridge width has to be smaller than  $2 \mu\text{m}$ .<sup>5,6</sup>

In conclusion, we have presented time-resolved emission spectra and far-field distributions along with theoretical computations which show that local self-heating of InGaN-based violet-blue diode lasers together with carrier diffusion effects can result in lateral mode switching and beam steering of the far field on a microsecond time scale. This unwanted behavior can be avoided if the ridge width is reduced to  $1.5 \mu\text{m}$ .

The financial support for the work at University of Ulm by the German government (BMBF) under contract Nos. 01BS151 and 01BS150 and by the Sofja Kovalevskaja Program of the Alexander von Humboldt Foundation is gratefully acknowledged. The work at OSRAM Opto Semiconductors is partly financed by the German government (BMBF) under contract No. 01BS150, and W. W. Chow is supported in part by the Humboldt Foundation and the US Department of Energy under contract No. DE-AC04-94AL85000.

<sup>1</sup>W. W. Chow and H. Amano, IEEE J. Quantum Electron. **37**, 265 (2001).

<sup>2</sup>V. Kümmler, G. Brüderl, S. Bader, S. Müller, A. Weimar, A. Lell, V. Härle, U. T. Schwarz, N. Gmeinwieser, and W. Wegscheider, Phys. Status Solidi A **194**, 419 (2002).

<sup>3</sup>C. Eichler, S. S. Schad, M. Seyboth, F. Habel, M. Scherer, S. Müller, A. Weimar, A. Lell, V. Härle, and D. Hofstetter, Phys. Status Solidi C **0**, 2283 (2003).

<sup>4</sup>K. J. Ebeling, *Integrierte Optoelektronik: Wellenleiter, Photonik, Halbleiter*, 2nd ed. (Springer, Berlin, 1992).

<sup>5</sup>S. Nakamura, M. Senoh, S. Nagahama, N. Iwasa, T. Yamada, T. Matsushita, H. Liyoku, Y. Sugimoto, and T. Kozaki, Jpn. J. Appl. Phys. **37**, L1020 (1998).

<sup>6</sup>T. Tojyo, S. Uchida, T. Mizuno, T. Asano, M. Takeya, T. Hino, S. Kijima, S. Goto, Y. Yabuki, and M. Ikeda, Jpn. J. Appl. Phys. **41**, 1829 (2001).